ELSEVIER

Atmospheric Research 53 (2000) 171–183

ATMOSPHERIC RESEARCH

www.elsevier.com/locate/atmos

Efficient computation of vapor and heat diffusion between hydrometeors in a numerical model

Robert L. Walko [a,*], William R. Cotton [a], Graham Feingold [a], Bjorn Stevens [b]

[a] *Department of Atmospheric Science, Colorado State University, Fort Collins, CO 80523 USA*
[b] *Department of Atmospheric Sciences, 405 Hilgard Avenue, Box 951565, Los Angeles CA 90095-1565, USA*

Abstract

We present an algorithm for representing diffusion of sensible heat and vapor between hydrometeors and air that is formulated from implicit numerical equations and is therefore stable for long numerical model timesteps, but is solved explicitly without requiring iteration. Liquid, ice, and mixed-phase hydrometeor categories are incorporated into the system, and latent heat of fusion released or absorbed during the diffusion process is accounted for. The method has been incorporated into the Regional Atmospheric Modeling System (RAMS) which prognoses ice–liquid potential temperature as its principal thermodynamic variable, but may be adapted to other models as well. Simulations with RAMS used as a parcel model are presented and demonstrate the performance of the new algorithm.

Keywords: Vapor diffusion; Heat diffusion; Implicit computation; Hydrometeor temperature

1. Introduction

Diffusive fluxes of vapor and sensible heat between hydrometeors and air are driven by differences in vapor mixing ratio and temperature, respectively, between the hydrometeor surfaces and air. Over an infintesimal time interval, each flux behaves as an interaction solely between an individual hydrometeor and the air. However, over a time step of seconds to minutes employed in most atmospheric numerical models, fluxes involving one hydrometeor category may alter air temperature and vapor mixing ratio

* Corresponding author. Fax: +1-970-4918449.
E-mail address: walko@atmos.colostate.edu (R.L. Walko).

0169-8095/00/$ - see front matter
PII: S0169-8095(99)00044-7

Table 1
List of symbols

A_1	$T_{il}\overline{L}/(C_p 253)$ for $T_{ac}^* < -20$°C; $T_{il}\overline{L}/[C_p(2T_a^* - T_{il})]$ for $T_{ac}^* > -20$°C
A_2	κA_1
A_3	$\kappa(T_{ac}^* + A_1 r_v^*)$
A_{4j}	$r'_{sRj}T_{Rj} - r_{sRj}$
A_{6j}	$L_j r'_{sRj}$
A_{8j}	$L_j A_{4j}$
B_j	$N_j(F_{Re})_j 4\pi\Delta t$
C_i	Specific heat of ice
C_l	Specific heat of liquid water
C_p	Specific heat of dry air at constant pressure
D_j	$H_j r_j^*$
E_j	$U_j A_{6j} + B_j\kappa$
F_j	$U_j L_j - B_j A_2$
$(F_{Re})_j$	Product of the ventilation coefficient, shape factor, and hydrometeor diameter integrated over the hydrometeor size spectrum of category j
G_j	$U_j A_{8j} + B_j A_3 + J_j Q_j^* r_j^* - V_j L_j r_j^* + \lambda_j$
H_j	0 for pristine ice, snow, and aggregates below 0°C and for cloud water; 1 for pristine ice, snow, and aggregates at 0°C, and for rain, graupel, and hail
i_g, i_h	Fraction of graupel, hail mass that is composed of ice
i_j	Fraction of mass in category j that consists of ice
j	Subscript denoting any particular hydrometeor category
J_j	0 for cloud water, pristine ice, snow, and aggregates; 1 for rain, graupel, and hail
K_j	0 for all-ice categories: pristine ice, snow, and aggregates; L_{il} for all-liquid categories: cloud water and rain
L_{il}	Latent heat of fusion
L_{iv}	Latent heat of sublimation
L_{lv}	Latent heat of evaporation
L_j	L_{lv} for liquid water categories; L_{iv} for ice water categories
$\overline{L}$	$q_{lat}^* / \Sigma_j r_j^*$
M_j	1 for all-liquid and all-ice cases; 0 for a mixed-phase hydrometeor
N_j	Number of hydrometeors of category j per m^3 of air
p	Atmospheric pressure
p_{00}	Reference pressure equal to 10^5 Pa
q_{lat}	Latent heat released in forming all condensate in a given volume from vapor
r_j	Mixing ratio of hydrometeor category j
r_{sj}	Water vapor mixing ratio at the surface of hydrometeors of category j, assumed to be at the saturation value with respect to hydrometeor temperature
r_{sl}	Saturation mixing ratio over water at air temperature T_{ac}
r_v	Water vapor mixing ratio
R	Gas constant for dry air
r_{sRj}	Saturation mixing ratio at T_{Rj} with respect to either liquid or ice,whichever is appropriate for category j
r'_{sRj}	Rate of change of r_{sRj} with temperature at T_{Rj}
S_j	$F_j/(C_j D_j + E_j)$
T_a	Air temperature in K
T_{ac}	Air temperature in °C
T_{il}	Ice–liquid temperature
T_j	Mean category temperature in °C
T_{Rj}	Reference temperature chosen to be close to $T_j^{t+\Delta t}$
$()^t$	Any quantity applying before dynamic tendencies

Table 1 (*continued*)

$\overline{()}^{*}$	Any quantity applying after dynamic tendencies but before diffusion
$()^{t+\Delta t}$	Any quantity applying after diffusion
U_j	ψBj if category j does not completely evaporate in the current timestep; 0 if category j completely evaporates in the current timestep
V_j	0 if category j does not completely evaporate in the current timestep; 1 if category j completely evaporates in the current timestep
W_j	$(G_j - K_j D_j)/(C_j D_j + E_j)$
Y_j	$r'_{sRj} W_j M_j - A_{4j}$
Z_j	$1 - r'_{sRj} S_j M_j$
θ_{il}	Ice–liquid potential temperature
κ	Thermal conductivity of air
λ	Sensible heat flux to hydrometeors by radiative transfer
ρ	Dry air density
ψ	Vapor diffusivity

sufficiently before the end of the timestep to affect fluxes involving the same or other categories occupying the same grid cell or parcel. Hence, in most numerical models, diffusion must be treated as an interactive process in which the thermodynamic state of each hydrometeor category influences all categories present. This is most true in the case of cloud droplets, which are so numerous that small changes in humidity can completely evaporate all droplets or nucleate a large number of new ones in a fraction of a timestep.

Hall (1980) discusses three numerical methods that have been applied to solving the diffusion equations. The explicit method evaluates and applies diffusion rates on a small timestep, bypassing the need to consider the system interactive. This method is prohibitively expensive computationally, requiring timesteps as small as 0.2 s (Arnason and Brown, 1971), and is therefore not practical for general modeling applications. The combined analytical/numerical method has been used successfully for liquid phase simulations by Clark (1973) and others, and involves calculating the timestep-averaged value of supersaturation, which is then applied to the hydrometeor growth equations. The implicit method was used by Hall (1980) who found it more suited to models containing both liquid and ice hydrometeors. This method involves driving vapor and heat diffusion by gradients that apply at the conclusion of the diffusion process, after hydrometeor and air temperature and water content are modified by diffusion. Such an implicit linear system is commonly solved by iterative methods, as was done in Hall (1980), or by other matrix solution methods.

This paper introduces an implicit method of computing vapor and heat diffusion between hydrometeors and air which was recently implemented and tested in the Regional Atmospheric Modeling System (RAMS). The method is similar to that employed by Hall (1980), but is solved in closed form without requiring iteration or matrix solution methods. Energy and water conservation equations are formulated in implicit numerical form for all hydrometeor categories and air. These are algebraically combined into a single predictive equation for future vapor mixing ratio of air (that applying after diffusive heat and water transfer) in which all terms on the right hand side are known and which is therefore evaluated explicitly. Future hydrometeor and air

temperatures, followed by diffusive vapor transfers, are all computed explicitly from the above result. The explicit, non-iterative form of the solution makes the method very efficient, as well as stable for long model timesteps.

Ice phase thermodynamics, especially involving latent heat of fusion, is treated by introducing hydrometeor internal energy as a prognostic variable in place of temperature. Heat budget equations for hydrometeors based on this variable easily incorporate freezing and melting, where hydrometeors maintain a temperature of 0°C when consisting of a mixture of liquid and ice. Sensible heat sources from hydrometeor collisions and radiative transfer are included. This form of the hydrometeor energy equations was used in an earlier version of RAMS (Walko et al., 1995; Meyers et al., 1997) in which cloud water mixing ratio was a diagnostic variable. In the present formulation, cloud water is prognostic and vapor and heat transfers are fully interactive between hydrometeor categories.

Section 2 describes the basic equations that govern conservation and transfer of energy and vapor, and how the equations are combined into a closed form. In order to keep the equation set compact at each stage of development, we introduce a large number of symbols, which are defined in Table 1. Section 3 shows application of the new formulation in RAMS.

2. Derivation

The equation set derived in this section contains a few elements that are specific to RAMS, particularly in its thermodynamic formulation and definition of hydrometeor categories, but could easily be adapted to other models. A comprehensive description of the RAMS bulk microphysics model is given in Walko et al. (1995) and Meyers et al. (1997). The following derivation replaces the vapor and heat diffusion equations developed in Walko et al. (1995), which did not include cloud water as a prognostic quantity and did not combine vapor and heat diffusion to different hydrometeor species into a single implicit system of equations.

We consider a volume of air of dry density ρ_a, pressure p, and temperature T_a (in Kelvins) or T_{ac} (in °C) that contains any or all of the following forms of water: vapor, cloud droplets, rain, pristine ice crystals, snow, aggregates, graupel, and hail, with mass mixing ratios relative to dry air denoted by r_v, r_c, r_r, r_p, r_s, r_a, r_g, and r_h, respectively. Graupel and hail only are allowed to consist of liquid and ice mixtures. The fraction of their mass that is composed of ice is represented by i_g and i_h. Any hydrometeor category may be denoted by subscript j; thus, r_j and T_j represent mixing ratio and temperature of any category. Hydrometeors in each category are assumed to conform to a generalized gamma size distribution described by Flatau et al. (1989) and Verlinde et al. (1990). RAMS prognoses mixing ratios r_j for all seven categories and, optionally, number concentration N_j as well. When N_j is not prognosed, it is normally specified for cloud droplets and diagnosed from mixing ratio and specified hydrometeor mean mass for other categories.

We shall develop equations for advancing one timestep in the numerical model, from time level t to $t + \Delta t$. Computation of vapor and heat diffusion between the hydromete-

ors and air are carried out with implicit time differencing, while other sources and sinks of heat and water, including transport, radiative absorption and emission, and collisions between hydrometeors of different categories, are computed using explicit differencing. Explicit processes other than radiation are carried out first, prior to heat and vapor diffusion, and result in partial updates of variables from time level t to a state denoted by an asterisk (*). Thus, T_{ac}^{*}, r_{v}^{*}, T_{j}^{*}, and r_{j}^{*} are the partially updated air temperature, vapor mixing ratio, hydrometeor temperature and hydrometeor mixing ratio, needing only radiation and vapor and heat diffusion to be fully updated to the future values $T_{ac}^{t+\Delta t}$, $r_{v}^{t+\Delta t}$, $T_{j}^{t+\Delta t}$, and $r_{j}^{t+\Delta t}$.

A cornerstone of the formulation is the use of ice–liquid potential temperature θ_{il} (in Kelvins) as a prognostic variable in RAMS (Tripoli and Cotton, 1981). θ_{il} is conservative in adiabatic motion and for internal water phase changes. Sources for θ_{il} in a parcel include turbulent mixing, radiative transfer, and addition or removal of hydrometeors by sedimentation. Air temperature is diagnosed by

$$T_a = T_{il}\left[1 + \frac{q_{lat}}{c_p \max(T_a, 253)}\right], \tag{1}$$

where

$$T_{il} = \theta_{il}\left(\frac{p}{p_\infty}\right)^{R/C_p} \tag{2}$$

may be called the ''ice–liquid temperature'' (in Kelvins), p_{oo} is a reference pressure of 1000 mb, R and C_p are the gas constant and specific heat at constant pressure for air, q_{lat} is the latent heat in Joules per kilogram of air that would be released in converting from vapor all liquid and ice that are contained in the parcel, and is given by

$$q_{lat} = \left[r_c + r_r + (1 - i_g) r_g + (1 - i_h) r_h\right] L_{lv} + \left(r_p + r_s + r_a + i_g r_g + i_h r_h\right) L_{iv}, \tag{3}$$

and L_{lv} and L_{iv} are the specific heats of evaporation and sublimation, respectively.

Eq. (1) may be written in the linearized form

$$T_{ac}^{t+\Delta t} - T_{ac}^{*} = A_1\left(r_{v}^{*} - r_{v}^{t+\Delta t}\right). \tag{4}$$

T_{ac} is evaluated from Eq. (1). A_1 is defined in Table 1 and is proportional to $\overline{L}$, which is the latent heat weighted between L_{iv} and L_{lv} according to the relative mixing ratios of liquid and ice contained in all hydrometeors. An approximation made in Eq. (4) is the application of $\overline{L}$ as an estimate for time level $t + \Delta t$, i.e., assuming that the ice-to-liquid ratio is not changed by the diffusion process. Any deviation from this assumption results in an error in $T_{ac}^{t+\Delta t}$ that is small for one timestep and does not accumulate to the next timestep. Eq. (4) represents latent heating (cooling) of air due to diffusion of water vapor to (from) hydrometeors. The net diffusional loss of water vapor is the net gain of water mass summed over all hydrometeor categories:

$$r_{v}^{*} - r_{v}^{t+\Delta t} = \sum_{j}\left(r_{j}^{t+\Delta t} - r_{j}^{*}\right). \tag{5}$$

The change in mixing ratio of category j over a model timestep due to vapor diffusion is given by

$$r_j^{t+\Delta t} - r_j^* = U_j\left(r_v^{t+\Delta t} - r_{sj}^{t+\Delta t}\right) - V_j r_j^* \tag{6}$$

(See Table 1 for definition of symbols). The term that contains U_j describes vapor diffusional growth or evaporation of a hydrometeor due to a vapor gradient between its surface and the ambient. Superscript $t+\Delta t$ in this term makes the equation implicit. In order to prevent evaporation during the timestep of more hydrometeor mass than is present, the loss of vapor is constrained to not exceed r_j^* by switching to alternate values of U_j and V_j as defined in Table 1.

The term $r_{sj}^{t+\Delta t}$ is eliminated from Eq. (6) by substituting the following linearized form of the Clausius–Clapeyron equation:

$$r_{sj}^{t+\Delta t} = r_{sRj} + r'_{sRj}\left(T_j^{t+\Delta t} - T_{Rj}\right). \tag{7}$$

T_{Rj} is a reference temperature computed by

$$T_{Rj} = T_{ac} - \min\left(25{,}700\left(r_{sl} - r_v\right)\right), \tag{8}$$

but limited to a maximum of 0°C for ice hydrometeors, r_{sRj} and r'_{sRj} are the saturation mixing ratio and its derivative with respect to temperature at T_{Rj}, and r_{sl} is the saturation mixing ratio over liquid at the air temperature T_{ac}. Eq. (8) was derived empirically and produces a reference temperature that is sufficiently close to $T_j^{t+\Delta t}$ for any atmospheric conditions encountered that the linearized Clausius–Clapeyron equation is a very good approximation. The added complexity of the quadratic form of the Clausius–Clapeyron equation advocated by Srivastava and Coen (1992) is thus unnecessary. With Eq. (7), Eq. (6) becomes

$$r_j^{t+\Delta t} - r_j^* = U_j\left[r_v^{t+\Delta t} - r_{sRj} - r'_{sRj}\left(T_j^{t+\Delta t} - T_{Rj}\right)\right] - V_j r_j^*. \tag{9}$$

Substituting Eq. (9) into Eq. (5) and rearranging gives:

$$r_v^{t+\Delta t} = \frac{r_v^* + \sum_j U_j\left[r_{sRj} + r'_{sRj}\left(T_j^{t+\Delta t} - T_{Rj}\right)\right] + \sum_j V_j r_j^*}{1 + \sum_j U_j}. \tag{10}$$

In order to compute the future hydrometeor temperature $T_j^{t+\Delta t}$, we requirea hydrometeor energy equation. The internal energy of hydrometeor category j in Joules per kilogram of hydrometeor mass may be defined by

$$Q_j = i_j C_i T_j + \left(1 - i_j\right)\left(C_l T_j + L_{il}\right). \tag{11}$$

Q_j is defined to be zero for pure ice at 0°C. The product $Q_j r_j$ is the internal energy of category j per kilogram of air. Q_j and $Q_j r_i$ are intensive quantities.

The heat budget equation for hydrometeor category j may be written in terms of Q_j as:

$$Q_j^{t+\Delta t} r_j^{t+\Delta t} - Q_j^* r_j^* = B_j \kappa\left(T_{ac}^{t+\Delta t} - T_j^{t+\Delta t}\right) + \lambda_j + \left(r_j^{t+\Delta t} - r_j^*\right)\left(L_j + Q_j^{t+\Delta t}\right). \tag{12}$$

The left hand side represents the change of internal energy of category j per kilogram of air in a timestep resulting from the diffusion processes and from radiation. The term that contains κ represents sensible heat diffusion, and λ_j represents the convergence of radiative flux onto category j. The remaining term represents the contribution from the transport of vapor to the hydrometeors and includes both latent and sensible heat. The vapor sensible heat term, $Q_j^{t+\Delta t}$ times the change in r_j, is very small compared to the latent heat term, but is included in the hydrometeor energy budget so that an exact balance between sensible heat diffusion (due to temperature differences), latent heat diffusion, and radiation will not cause a change in Q_j. The vapor sensible heat term has a negligible direct effect on air temperature and is therefore not included in Eq. (4).

Rearranging Eq. (12) gives:

$$\left(Q_j^{t+\Delta t} - Q_j^*\right) r_j^* = B_j \kappa \left(T_{ac}^{t+\Delta t} - T_j^{t+\Delta t}\right) + \lambda_j + \left(r_j^{t+\Delta t} - r_j^*\right) L_j. \tag{13}$$

The model-predicted Q value is stored from one timestep to the next for the more massive hydrometeor categories, rain, graupel, and hail, so that the liquid water content of graupel and hail may be predicted and rain temperature is allowed to be out of equilibrium with atmospheric temperature and humidity, as immediately after being formed from melted ice or shed from hail. For these categories, Q_j^* is therefore known and the full heat budget Eq. (13) is evaluated. The remaining categories (cloud droplets, pristine ice, snow, and aggregates) are assumed to have negligible heat storage capacity and are not allowed to retain a mixture of liquid and ice from the previous timestep. For cloud droplets or for ice below 0°C, this implies a balance between sensible and latent heat diffusion and radiation. Thus, Q_j^* is equal to $Q_j^{t+\Delta t}$ and the terms on the right hand side of Eq. (13) sum to zero. For ice undergoing melting, Q_j^* is set to zero and $Q_j^{t+\Delta t}$ is evaluated from Eq. (13).

Taking the appropriate case for each category and substituting Eq. (4) into Eq. (13) to eliminate $T_{ac}^{t+\Delta t}$, and from Eq. (9) into Eq. (13) to eliminate $r_j^{t+\Delta t}$ gives, after rearranging:

$$Q_j^{t+\Delta t} D_j + T_j^{t+\Delta t} E_j = r_v^{t+\Delta t} F_j + G_j. \tag{14}$$

Eq. (11) is applied for each hydrometeor category to eliminate $Q_j^{t+\Delta t}$ from Eq. (14): For all-liquid categories (cloud droplets and rain), $Q_j^{t+\Delta t} = C_l T_j^{t+\Delta t} + L_{il}$. For all-ice categories, $Q_j^{t+\Delta t} = C_i T_j^{t+\Delta t}$. For any ice category in mixed-phase, including pristine ice, snow, and aggregates undergoing melting, $T_j^{t+\Delta t} = 0$°C; this case will be considered later. The all-liquid and all-ice cases may be written as

$$Q_j^{t+\Delta t} = C_j T_j^{t+\Delta t} + K_j, \tag{15}$$

where K_j is L_{il} for all-liquid categories and 0 for all-ice categories and C_j is C_l or C_i as appropriate for category j.

Substituting Eq. (15) into Eq. (14) gives the following equation for $T_j^{t+\Delta t}$:

$$T_j^{t+\Delta t} = \left[S_j r_v^{t+\Delta t} + W_j\right] M_j. \tag{16}$$

Whether M_j is 0 or 1 for an ice category is estimated beforehand by applying Eq. (16) with $M_j = 1$ and assuming that $r_v^{t+\Delta t}$ equals r_v^t, its value on the previous timestep, or that it equals $2r_v^t - r_v^{t-\Delta t}$, an extrapolation from the previous two timesteps. If $T_j^{t+\Delta t} \geq 0$ results from this trial, the category is taken to be at 0°C and M_j is set to 0, while if $T_j^{t+\Delta t} < 0$, M_j is set to 1. For pristine ice, snow, and aggregates, the trial is performed with $H_j = 0$. If the category is found to be at 0°C, then H_j is set to 1.

Hydrometeor temperature $T_j^{t+\Delta t}$ given by Eq. (16) is substituted into Eq. (10) which gives, after rearrangement:

$$r_v^{t+\Delta t} = \frac{r_v^* + \sum_j U_j Y_j + \sum_j V_j r_j^*}{1 + \sum_j U_j Z_j}. \tag{17}$$

Eq. (17) provides a closed solution for $r_v^{t+\Delta t}$ in which the fast-response phenomena (diffusion of vapor and heat between hydrometeors and air and associated temperature responses of hydrometeors and air) are implicitly balanced, slower phenomena, including transport, hydrometeor collisions, and radiative transfer, are represented as explicit forcing terms (in terms with the asterisk (*) symbol), and the effects of heat storage and latent heat of fusion in hydrometeors are included where appropriate. All terms on the right hand side are known prior to diffusion, and therefore Eq. (17) may be evaluated explicitly without iteration. With $r_v^{t+\Delta t}$ determined, $T_j^{t+\Delta t}$ is evaluated for each category from Eq. (16). The change in mixing ratio of each category is evaluated from Eq. (9).

In first computing $r_v^{t+\Delta t}$ from Eq. (17), it is assumed that no hydrometeor categories completely evaporate, and that consequently $U_j \neq 0$ and $V_j = 0$. If it is found from evaluating Eq. (9) that a category completely evaporates, U_j and V_j are changed to their alternate values, $r_v^{t+\Delta t}$ is corrected appropriately from Eq. (17), and $r_j^{t+\Delta t}$ is set to zero for that category. This is done in the following order: cloud droplets, pristine ice, aggregates, snow, rain, graupel, and hail, starting with the categories whose evaporation rate is potentially the largest and could therefore have the largest impact on the other categories.

Once $r_v^{t+\Delta t}$, $T_j^{t+\Delta t}$, $r_j^{t+\Delta t}$, U_j, and V_j are all determined, $Q_j^{t+\Delta t}$ is evaluated either from Eq. (15) in any case where $M_j = 1$, or from Eq. (14) in cases where $M_j = 0$, including pristine ice, snow, and aggregates undergoing melting. $Q_j^{t+\Delta t}$ determines temperature and liquid water content which are used in deciding how mass and number are transferred between categories in hydrometeor collisions, melting of ice, and shedding of rain by hail. Air temperature is evaluated from Eq. (4).

In most circumstances, the trial value of M_j used in Eq. (16) will be correct. However, occasionally when an ice hydrometeor has a Q value very near zero and the value of $r_v^{t+\Delta t}$ predicted from Eq. (17) deviates sufficiently from the estimate used in Eq. (16) to determine M_j, or where graupel and hail transition from mixed-phase to completely frozen during the current timestep, M_j may be set incorrectly. If M_j should be 0 but is set to 1, the ice temperature predicted by Eq. (16) and implicit in Eq. (17) will be slightly above 0°C resulting in more diffusion of heat and vapor to the air should actually occur. While this error is usually small, its effect on atmospheric vapor and

temperature is bounded in any case by the prevention of overevaporation of any category. Ice internal energy predicted by Eq. (14) would be too low, so it is limited to zero in such cases.

If M_j should be 1 but is set to 0, the ice temperature predicted by Eq. (16) and implicit in Eq. (17) will be 0°C, which is again be slightly warmer than it should be. Ice internal energy predicted by Eq. (15) is zero in this case, which is very close to the correct value so no limits need be applied.

3. Model tests and verification

The most fundamental and important level of testing the formulation of Section 2 is to verify that all equations are satisfied in the model solution, particularly those that are not directly evaluated in the model. For example, RAMS does not directly evaluate Eq. (5) describing the conservation of total water, but instead computes $r_v^{t+\Delta t}$ from Eq. (17) and $r_j^{t+\Delta t}$ from Eq. (9). For testing, we thus evaluate Eq. (5) to verify that it is satisfied for all cases. Similarly, Eq. (6) describing vapor transfer to category j, Eq. (7) describing the surface vapor mixing ratio, and Eq. (12) describing the hydrometeor energy budget are all tested in model simulations for conformity to machine accuracy. These tests have confirmed that all physical processes represented in the equations are carried out accurately.

A full validation of RAMS microphysics results against other models and observations necessarily involves all other microphysical (and dynamical) processes, which are beyond the scope of this paper, and other applications of the model have made such comparisons. Here, we instead show results from two simple simulations in which RAMS is run as a parcel model. This helps to isolate the physical processes described Section 2.

In the first simulation, a parcel initially at a temperature of 14 K and relative humidity of 80% ascends at approximately 6 m s^{-1} for 2000 s. During this time, the parcel cools and saturates, producing cloud water and later pristine ice crystals, the only two condensate categories allowed in this simulation. Sedimentation is turned off in order to examine conservation properties of the parcel, and both hydrometeor collisions and freezing of cloud droplets are turned off so that all mass transfer between cloud and ice is through vapor flux. A timestep of 10 s is used.

Time series of various microphysical and thermodynamic quantities are shown in Fig. 1. Relative humidity with respect to liquid increases rapidly and reaches saturation at about 80 s. An episode of supersaturation of a few percent occurs in one timestep before cloud droplets are present to absorb water vapor. Such high supersaturation is unrealistic, of course, and will be remedied in the future by introducing a cloud nucleation model that implicitly produces and grows cloud droplets as soon as critical supersaturation is reached. At the end of this timestep, having achieved supersaturation, cloud droplets are introduced with a specified concentration of 10^9 per kg of air. On the following timestep, vapor flux to the droplets begins, and peaks because of the excess vapor produced on the previous timestep. For the following few hundred seconds, cloud water grows at the expense of vapor at a smooth but decreasing rate as the air dries.

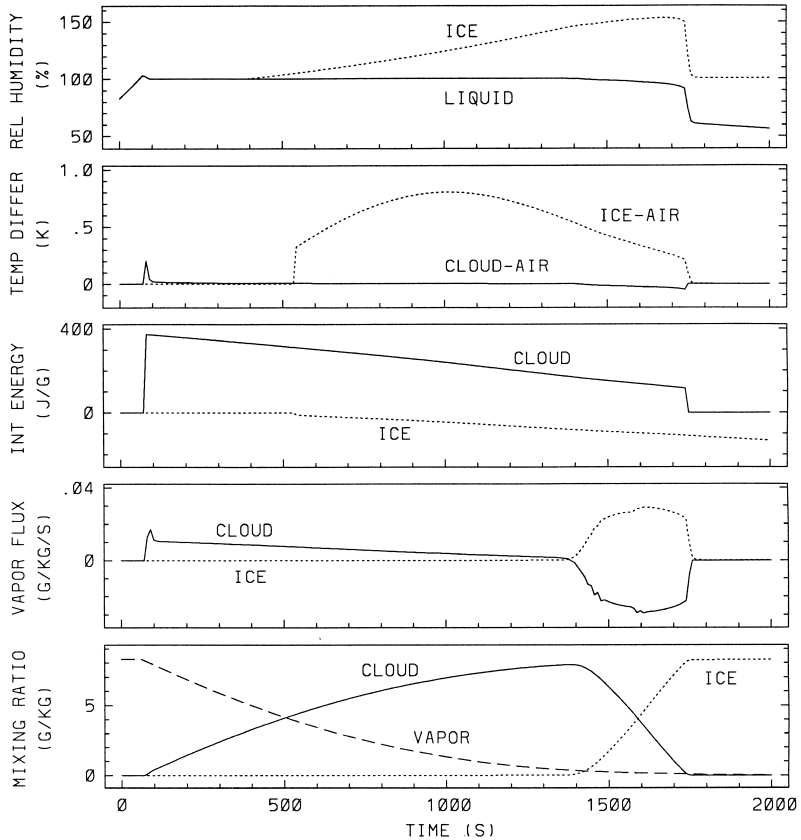

Fig. 1. Relative humidity (%) with respect to liquid and ice; ice–air and cloud–air temperature differences (K); cloud and ice internal energies (J g^{-1}); vapor fluxes to cloud and ice hydrometeors (g kg^{-1} s^{-1}); and mixing ratios of cloud, ice, and vapor (g kg^{-1}) as a function of simulation time (s) for parcel simulation case 1.

Cloud water is slightly warmer than the air during this time due to latent heat of condensation. The spike in the cloud-air temperature difference near 80 s is another artifact of the sudden diffusion of excess vapor at cloud initiation that will be corrected with the cloud nucleation model. Internal energy of cloud water is computed once cloud water appears and begins near 380 J g^{-1}, followed by a steady decline. A value of 334 J g^{-1} corresponds to a liquid temperature of 0°C, which is reached by cloud water (and air) near 400 s.

Ice crystals begin forming at 540 s when the air temperature reaches -5°C, a feature of the ice nucleation parameterization in the model. Once formed, they begin absorbing vapor, and maintain a temperature a few tenths of a Kelvin above the air temperature due to latent heat release. This temperature difference is much larger than for cloud water because supersaturation with respect to ice, and hence vapor flux to ice, is much larger per individual hydrometeor. The number of ice crystals remains so low for several

hundred seconds that the overall vapor flux to ice is far less than to cloud water, however.

Near 1400 s, ice crystals are sufficiently numerous and large that vapor flux to ice becomes large. The relative humidity of air with respect to liquid falls a few percent below saturation and cloud water begins to rapidly evaporate. As a result, cloud water temperature drops to a few hundredths of a Kelvin below air temperature. However, as ice is rapidly growing by vapor deposition, it remains a few tenths of a Kelvin warmer than air. Near 1750 s, cloud water is completely evaporated, and ceases to maintain a vapor supply near saturation with respect to liquid. Vapor flux continues to ice until the air dries to saturation with respect to ice. The internal energy of ice continues to fall steadily from the time ice forms. The slope of this decrease is half that exhibited by cloud water because the specific heat of ice is half that of liquid.

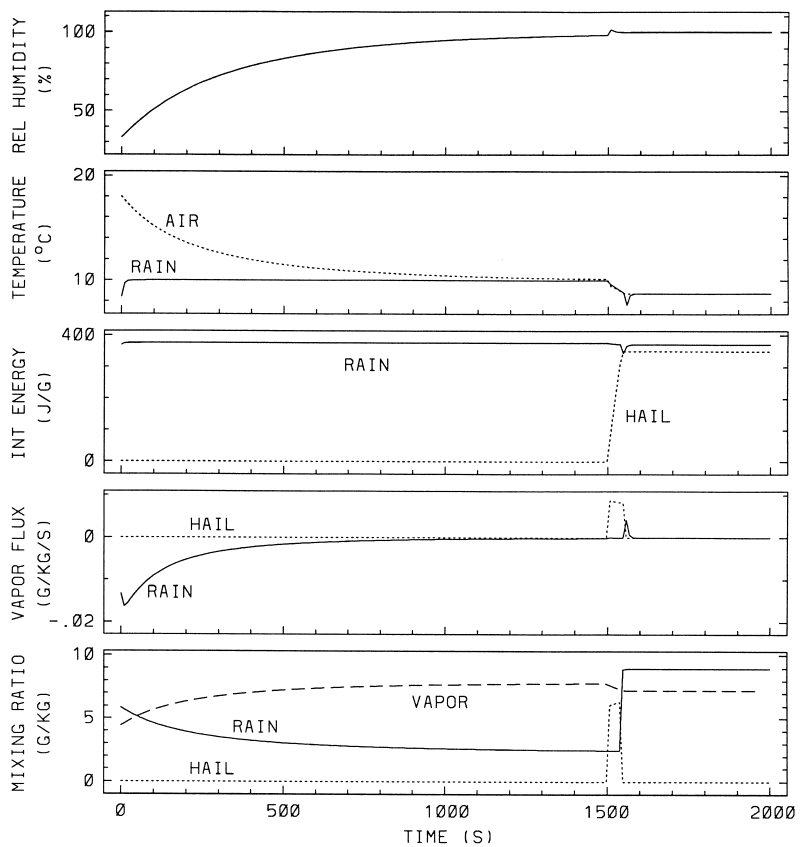

Fig. 2. Relative humidity (%) with respect to liquid; rain and air temperatures (°C); rain and hail internal energies (J g^{-1}); vapor fluxes to rain and hail (g kg^{-1} s^{-1}); and mixing ratios of rain, hail, and vapor (g kg^{-1}) for parcel simulation case 2.

In the second simulation, the parcel is initially at 18°C and 30% relative humidity, and remains at constant height. On the first timestep, 6 g kg^{-1} of rain is added suddenly, as if falling into the parcel from above. The rain is not permitted to fall out of the parcel, but it does keep its ventilation coefficient as if falling at its natural velocity. The rain is given an initial temperature of 0°C as if it were just shed or melted from hail.

Time series of several quantities from this simulation are shown in Fig. 2. At the end of the first (10-s) timestep, sensible heat diffusion has elevated the rain temperature to about 8°C, even though evaporative cooling of rain is also occurring. The vapor flux rate from rain is about .012 g kg^{-1} on the first timestep. On the next few timesteps, rain continues to warm until relaxing to the wet bulb temperature of 10°C. The vapor flux rate reaches its extreme value during this time. Up to simulation time 1500 s, rain continues to evaporate at the wet bulb temperature, air vapor accordingly increases, and air temperature decreases, asymptotically approaching the wet bulb temperature. Relative humidity becomes very close to 100% by this time, and consequently the dew point temperature and air temperatures converge to the wet bulb temperature of 10°C.

Hail with a mean-mass diameter of 2 mm and mixing ratio of 6 g kg^{-1} is introduced into the parcel at 1500 s, and is prevented from falling out of the parcel as for rain. The internal energy of hail is initially 0 J kg^{-1}, representing a temperature of 0°C and 100% ice content. Because hail is below the air and dew point temperatures, sensible heat and vapor both diffuse to hail, rapidly increasing its internal energy. From 1500 to 1550 s, hail increases in mixing ratio by 0.4 g kg^{-1} due to vapor deposition. However, by 1550 s, the large amount of latent heat of condensation released plus the sensible heat diffused to hail have increased its internal energy to 334 J kg^{-1}, indicating complete melting. Hail is then converted to rain, which temporarily lowers the rain temperature and initiates vapor and sensible heat flux to rain until its temperature returns to the wet-bulb value. Air and rain both cool by 0.6°C during the time hail exists as a result of the sensible heat transfer to hail.

4. Summary

The solution derived in this paper for computing fully interactive transfers of sensible heat and vapor between hydrometeors, along with associated hydrometeor and air temperatures, is stable, efficient by requiring no iteration, and is reasonably accurate for long timesteps. It has been successfully implemented and used in the RAMS, and should be easily adaptable to other models as well.

Basic numerical tests of the equation set and its solution confirm that the component equation representing the temperature and mixing ratio change of air and each hydrometeor class is satisfied to machine precision. Simulation tests using RAMS as a parcel model demonstrate that the overall behavior of the system is physically realistic.

The solution includes a supersaturation computation that is suitable for driving a cloud activation model which would predict cloud droplet number given a CCN population and characteristics. Such a model is not yet fully tested and will be the topic of a future paper.

Acknowledgements

The first two authors wish to thank Professor Zev Levin of the University of Tel Aviv, Professor Alexander Khain of the Hebrew University of Jerusalem, and the Israel Science Foundation for inviting us to present this work at the International Research Workshop of the Israel Science Foundation on Trends and Advances in Numerical Modeling of Clouds and Precipitation, at Kibbutz Ginosar, Israel, 17–20 November, 1997. The International Workshop was supported by both universities and by the Israel Academy of Science. This research was supported under National Science Foundation grant ATM-9529321, National Oceanic and Atmospheric Administration grant NA67RJ0152, and Department of Energy grant DE-FG03-95ER61958.

References

Arnason, G., Brown, P.S., 1971. Growth of cloud droplets by condensation: a problem in computational stability. J. Atmos. Sci. 28, 119–143.

Clark, T.L., 1973. Numerical modeling of the dynamics and microphysics of warm cumulus convection. J. Atmos. Sci. 30, 857–878.

Flatau, P.J., Tripoli, G.J., Verlinde, J., Cotton, W.R., 1989. The CSU-RAMS cloud microphysical module: general theory and code documentation. Colorado State University, Dept. of Atmospheric Science, Fort Collins, CO 80523. Atmos. Sci. Pap. 451, 88 pp.

Hall, W.D., 1980. A detailed microphysical model within a two-dimensional dynamic fremework: Model description and preliminary results. J. Atmos. Sci. 37, 2486–2507.

Meyers, M.P., Walko, R.L., Harrington, J.Y., Cotton, W.R., 1997. New RAMS cloud microphysics parameterization: Part II. The two-moment scheme. Atmos. Res. 45, 3–39.

Srivastava, R.C., Coen, J.L., 1992. New explicit equations for the accurate calculation of the growth and evaporation of hydrometeors by the diffusion of water vapor. J. Atmos. Sci. 49, 1643–1650.

Tripoli, G.J., Cotton, W.R., 1981. The use of ice–liquid water potential temperature as a thermodynamic variable in deep atmospheric models. Mon. Wea. Rev. 109, 1094–1102.

Verlinde, J., Flatau, P.J., Cotton, W.R., 1990. Analytical solutions to the collection growth equation: comparison with approximate methods and application to cloud microphysics parameterization schemes. J. Atmos. Sci. 47, 2871–2880.

Walko, R.L., Cotton, W.R., Meyers, M.P., Harrington, J.Y., 1995. New RAMS cloud microphysics parameterization: Part I. The single-moment scheme. Atmos. Res. 38, 29–62.